International Journal of Engineering and Geosciences
https://dergipark.org.tr/en/pub/ijeg
e-ISSN 2548-0960

A comprehensive analysis of different geometric correction methods for the Pleiades -1A and Spot-6 satellite images

Buğrahan Özcihan [1], Levent Doğukan Özlü [1,2], Mümin İlker Karakap [1], Halime Sürmeli [2], Ugur Alganci [1], Elif Sertel [*1]

[1]*Istanbul Technical University, Civil Engineering Faculty, Geomatics Engineering Department, Istanbul, Türkiye*
[2]*Turkish Aerospace Industries, Inc. (TAI), Ankara, Türkiye*

Keywords
Remote Sensing
Geometric Correction
Accuracy Analysis
Empirical Models
Physical Models

Research Article
DOI: 10.26833/ijeg.1086861

Received: 13.03.2022
Accepted: 14.05.2022
Published: 19.10.2022

Abstract

Satellite images have been widely used in the production of geospatial information such as land use and land cover mapping and the generation of several thematic layers via image processing techniques. The systematic sensor and platform-induced geometry errors influence images acquired by sensors onboard various satellite platforms. Thus, geometric correction of satellite images is essential for image pre-processing to extract accurate and reliable locational information. Geometric correction of satellite images obtained from two different satellites, Pleiades 1A (PHR) and SPOT-6, was performed within the scope of this study using empirical models and a physical model. The 2D polynomial model, 3D rational function model with calculated RPCs from GCPs, 3D rational function model with RPCs from satellite, RPC refinement model using GCPs, and Toutin's physical model were used. Several experiments were carried out to investigate the effects of various parameters on the performance of the geometric correction procedure, such as GCP reference data source, GCP number and distribution, DEM source, spatial resolution, and model. Our results showed that lower RMSE values could be achieved with the model that uses RPC from data providers for PHR and SPOT, followed by the RPC refinement method for PHR and Toutin method for SPOT. In general, GCPs from the HGM data source and ALOS DEM combination provided better results. Lastly, lower RMSE values, thus better locational accuracy values, were observed with the PHR image except for a single test.

1. Introduction

Geospatial data is widely used in many disciplines for various purposes, including combating global warming, developing location-based services and navigation maps, producing thematic maps for city and regional planning, and estimating crop yield [1-8].

Remote sensing platforms provide a wide range of spatial data with different technical characteristics. However, a remote sensing image, which allows us to access up-to-date geographical information quickly, may contain geometric distortions caused by Earth's curvature, topographical conditions, and sensor data acquisition geometry. Before any further analysis of a remotely sensed image, pre-processing is required to obtain accurate and reliable geo-information [9-10]. Preprocessing is divided into two-fold: radiometric correction and geometric correction. Detector-based radiometric problems in images causing unexpected reflections are removed during the radiometric correction. Geometric correction is the process of minimizing the geometric distortions and defining the image in a specific coordinate system and datum [10-11]. According to Toutin [12], geometric distortions are commonly present in remotely sensed images. Therefore, it is necessary to geometrically correct images to reliably use them as a base map in a geographic information system (GIS), conduct accurate angle and distance measurements from these images or generate a precise spatial database of different features [13].

* **Corresponding Author**

(ozcihan17@itu.edu.tr) ORCID ID 0000-0002-4540-3140
(ozlul17@itu.edu.tr) ORCID ID 0000-0001-7121-8101
(karakap16@itu.edu.tr) ORCID ID 0000-0002-7128-2100
(halimerek@gmail.com) ORCID ID 0000-0002-7430-183X
(alganci@itu.edu.tr) ORCID ID 0000-0002-5693-3614
*(sertele@itu.edu.tr) ORCID ID 0000-0003-4854-494X

Cite this article

Özcihan, B., Özlü, L. D., Karakap, M. İ., Sürmeli, H., Algancı, U., & Sertel, E. (2023). A comprehensive analysis of different geometric correction methods for the Pleiades -1A and Spot-6 satellite images. International Journal of Engineering and Geosciences, 8(2), 146-153

Since the geometric correction of satellite images is a vital step for many remote sensing-based applications, several researches have been conducted on the analysis of different models' performance and accuracy by considering the effects of used digital elevation models (DEM), and ground control points (GCP).

Alganci et al. [14] emphasized the importance of appropriate DEM selection considering the purpose and scale of the study because DEM accuracy directly affects individual calculations and process chains. DEM's accuracy is very effective and important for geometric correction operations. In addition to the DEM's accuracy, the topographic characteristics of the study area are also impacting the performance of geometric correction processes. According to results in the same study, elevation values obtained from SPOT and PHR DSM's were better than SRTM, ALOS, and ASTER data. ALOS DSM provided significantly better results than other freely available DEMs. ASTER GDEM, which has a 30-m spatial resolution and is freely available, is also used in many studies of geometric correction.

Ground Control Points (GCP) also play an important role in geometric correction accuracy [9,15]. According to Samadzadegan et al., [16], the number and distribution of the ground control points highly affect the accuracy of geometric correction model results. The necessity of the homogeneous distribution of GCPs is clearly stated in previous research. Furthermore, the number of GCPs required varies depending on the mathematical model used. According to Toutin [12], the 2D/3D non-parametric models are sensitive to GCP's distribution and need many GCPs (>20-60), while 3D parametric models are not that sensitive to distribution and need few GCPs (3-8).

Besides DEM and GCPs, mathematical models are one of the main important components of the geometric correction process. In the study of Samadzadegan et al. [16], the DLT model, RFM, and Affine models were applied to SPOT, IRS, and IKONOS satellite images and according to the results, RFM provided better results than the other models. In another study by Kartal et al. [11], empirical models, which are the rational function model (RFM), RPC Refinement model and physical Toutin model, were applied to Pleiades images. ASTER GDEM was used for the ortho-rectification process. The physical Toutin model provided the highest accuracy in both study areas, followed by the first-order Rational Polynomial Coefficient (RPC) refinement model. They concluded that it is important to have sensor parameters to perform successful correction to imagery and non-parametric models are not as accurate as parametric models. Toutin [12], stated that 2D/3D polynomial nonparametric functions do not reflect the source of distortions thus they can be used only for images with small distortions, and they are also very sensitive to input errors like unsuitably distributed GCPs. According to the same study, the 3D rational function, which is also a non-parametric function, provides better accuracy than polynomial functions but is lower than parametric functions.

In another study on geometric correction, Ye et al. [17] performed geometric corrections on very high-resolution WorldView-2 satellite images (0.5m) with different models and compared the results. They used a physical model and RFM models, RPCs provided by the data provider, RPCs calculated by Least Square iterative method, and RPCs calculated by Correcting Characteristic Value method. Their results provided that both methods used in RPC calculation yielded more successful results than the coefficients provided by the metadata, and the CCVM method gave slightly more accurate results than the LS method. It was observed that the physical model gave better results than the model using the RPC coefficients provided by the provider, but fell behind the two methods performed by RPC calculations.

Son et al. [18] proposed an iterative precision geometry correction approach by implementing an image pyramid including GCP chip matching, outlier detection, and precise sensor modeling for the automatic detection of GCPs. They utilized their proposed approach to KOMPSAT-3 images and obtained average geometric accuracy of 1.5 pixels and a maximum of 2 pixels.

Zhang et al. [15] evaluated the geolocation accuracy of the Chinese First Polar Microsatellite (Ice Pathfinder, BNU-1) Imagery. The geometric calibration model of BNU-1 did not achieve good accuracy metrics due to the inaccuracy of satellite attitude and orbit parameters, which have to be precisely determined for a sensor-based calibration model. They used MODIS images to extract accurate GCPs and used them to correct the geolocation errors of BNU-1 images. They applied their methodology to Twenty-eight images of Antarctica and fifteen images of Arctic regions and improved the geometric correction accuracy from 10 km to 300m.

Mezouar et al. [19] performed a particle swarm optimization method-based approach to optimize the FRM over Alsat -2 images and reported an accuracy improvement between 21% and 38% over state-of-the-art approaches.

To obtain sub-pixel geometric accuracy, Misra et al. [20] proposed a feature detection approach based on mode-guided tiled scale-invariant feature transform (MT-SIFT) in hierarchical stages. They evaluated their automatic approach for Resourcesat multispectral camera images of different landscapes. They achieved the root mean square error (RMSE) of 0.12 pixels at a spatial resolution of 5 m.

A very current study by Wang et al. [21] proposes orthorectification of GF-3 SAR images using RPC files and TPs generated by SIFT algorithm. Their GCP-free experiment resulted in a mean RMSE of 0.724 pixels among 1,468 images.

By contemplating the important and dominant factors of geometric correction from the above literature, this study aims to comprehensively evaluate empirical and physical geometric correction models on high (HR) and very high-resolution (VHR) satellite images of Istanbul, Turkey. The effects of the freely available DEM sources, quantity and quality of GCPs, and spatial resolution of the satellite images on geometric correction models are investigated within this scope. The remainder of the paper is organized as follows. Section 2 provides detailed information about the study region and used datasets; Section 3 gives a detailed explanation of methods and analysis workflow, Section 4 presents

quantitative results, and Section 5 provides concluding remarks.

2. Study Area and Data

Within the scope of this study, satellite images of Istanbul were obtained from two different satellite platforms to be geometrically corrected using DEM and GCP data obtained from different sources. In this sense, the data used is presented under three subheadings: satellite imagery, ground control points and digital elevation models.

2.1. Satellite Imagery

This study investigates the performance of empirical and physical geometric correction methods on HR and VHR satellite images, obtained from SPOT-6 and Pleiades (PHR) satellites (Figure 1).

Pleiades 1A and 1B are VHR twin satellites, with a native spatial resolution of 0.7 meters for panchromatic and 2.8 meters for multispectral sensors. The products delivered by the provider are processed and resampled to 0.5m for panchromatic and 2.0m for multispectral images. A PHR image covers an area of approximately 20 km^2 on the ground. In this study, we used a Pleiades image covering the south-eastern part of the European side of Istanbul and captured on 15.05.2020.

SPOT-6 and SPOT-7 are twin satellites, with a spatial resolution of 1.5 meters for panchromatic and 6 meters for multispectral sensors. We used a SPOT-6 image of the European side of Istanbul, which was captured on 07.06.2020.

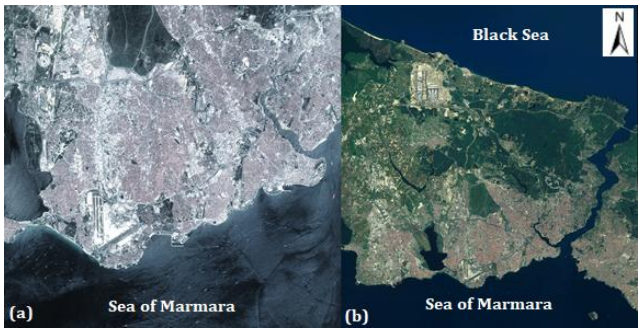

Figure 1. Preview of used satellite images a) PHR, b) SPOT

2.2. Ground Control Points

Ground Control Point (GCP) is very important to improve the accuracy of a satellite image. As mentioned in the literature review, in geometric correction studies, GCPs are very effective in obtaining better results. Checkpoint (CP) is the GCP that is not included in the process and is used to control how accurate the result of the process is. The following platforms were used as GCP and CP sources: 40 points from Google Earth (GE) as GCP and 20 points from General Directorate of Mapping (HGM) of Turkey as CP within this study.

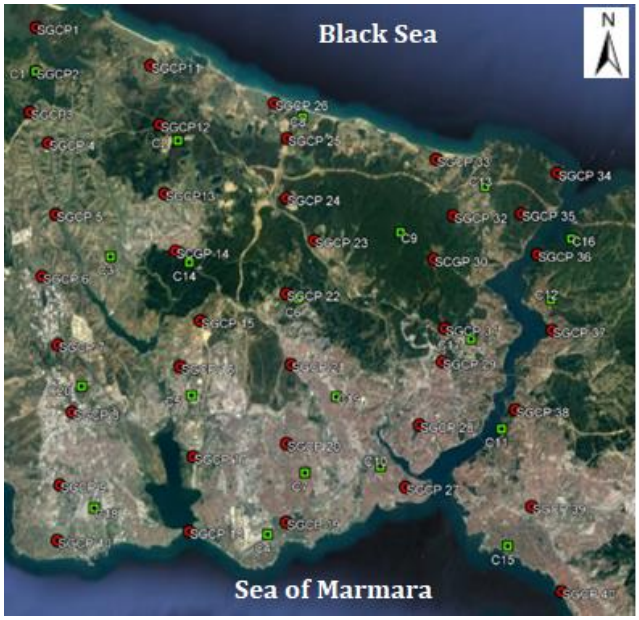

Figure 2. Distribution of GCPs (red) and CPs (green) in the study region

2.3. Digital Elevation Models

A Digital Elevation Model (DEM) represents the ground surface elevations with respect to any reference datum. DEM is a commonly used abstract model for the digital representation of topography. As DEM sources, we used Advanced Land Observing Satellite (ALOS), Advanced Spaceborne Thermal Emission and Reflection Radiometer Satellite (ASTER), and Shuttle Radar Topography Mission (SRTM) platforms in this study (2018).

The ALOS DEM has 30 meters spatial resolution. In the study of Alganci et al. [14], which evaluated the accuracy of DEMs for the same study region, the RMSE value of ALOS DEM was computed as 2.14 meters, and the accuracy value was calculated as 4.19 meters. ALOS DEM has the least RMSE value and is the most accurate among the other freely available DEMs. ASTER has 30 meters of spatial resolution, and it provides an RMSE value of 5.72 meters with an accuracy of 11.21 meters. SRTMDEM is the last DEM used in this study, which also has 30 meters spatial resolution. In the same study by Alganci et al., [14], the RMSE value of SRTM DEM was computed as 3.53 meters, and accuracy was calculated as 6.92 meters.

3. Methodology

In this study, we thoroughly examined both dependent and independent sensor models and then compared the results of different models. In addition, we also employed a physical model known as the Toutin Model. All processing, analysis and accuracy assessment procedures were performed with the PCI Geomatica software. A flowchart of the process chain is provided in Figure 3.

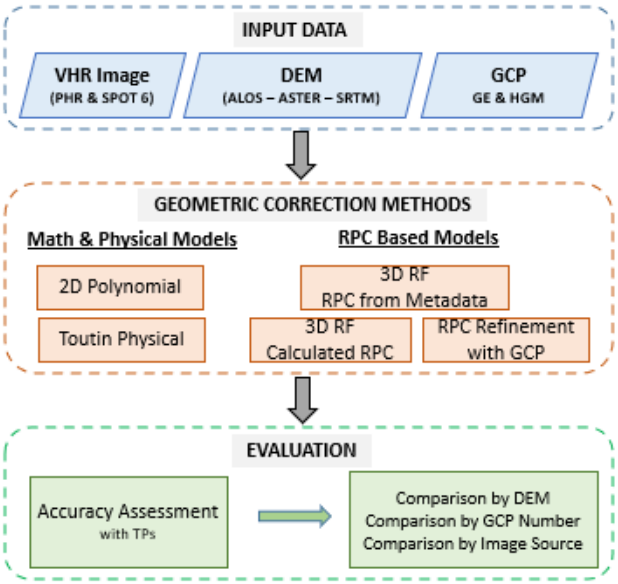

Figure 3. Methodological flowchart

3.1. 2D Polynomial Model

Polynomial models are used to transform between coordinate systems. The basic working principle of the 2-dimensional polynomial model is to establish a mathematical relationship between the pixel coordinates of the ground control points and the known ground coordinates. The degree of polynomial function may vary depending on the field conditions, the number of GCPs, and the targeted accuracy. Although a more accurate polynomial model is formed as the degree of polynomial increases, higher-order polynomials can create large distortions in parts of the image that do not have GCP [22]. In this study, 2nd order polynomial transformation is used.

Since surface topography variations are not considered in the 2-dimensional polynomial model, it is more appropriate to use it in flatlands where the height factor does not have a significant effect. The basic transformation function can be represented as Eq. 1 [13,23].

$$P_{2D}(XY) = \sum_{i=0}^{m}\sum_{j=0}^{n} a_{ij} X^i Y^j \qquad (1)$$

3.2 3D Rational Functional Model with Calculated RPCs

The Rational Function Model (RFM) is a mathematical model that correlates the pixels in the satellite image and their actual positions on the earth. Since the RFM uses height information of GCPs obtained from the DEM data used, it offers higher accuracy than polynomial models [24]. The x and y parameters are calculated by proportioning the two polynomial functions. The most significant advancement for RFM is working as a sensor-independent model by generating the RPC (Rational Polynomial Coefficient) from GCPs, which now include height information using DEM. The RFM structure is provided in Eq. 2 [13,23].

$$R_{3D}(XYZ) = \frac{\sum_{i=0}^{m}\sum_{j=0}^{n}\sum_{p=0}^{k} a_{ijk}X^iY^jZ^k}{\sum_{i=0}^{m}\sum_{j=0}^{n}\sum_{p=0}^{k} a_{ijk}X^iY^jZ^k} \qquad (2)$$

3.3. 3D Rational Functional Model with RPCs From Satellite

In addition to RPCs calculated from GCPs, RPCs provided by satellite companies to users within metadata can be used in the RFM model implementation [25]. These RPC files usually contain 20 numerator and denominator polynomial coefficients for the direct and inverse rational functional model. Although RPCs can be produced in different ways, they are mostly produced by the non-linear least square method to derive mathematical models that reflect the acquisition geometry.

3.4. RPC Refinement Model Using GCPs

After the RPC based geometric correction, the results could contain biases and random errors due to topography and sensor characteristics. To improve the results of the RPC model and eliminate the biases and random errors, a refinement function can be used together with GCPs [26]. The refinement functions are defined as:

$$Line_i^{(j)} = \Delta p^{(j)} + p^{(j)}(\Phi_k, \lambda_k, h_k) + \varepsilon_{Li} \qquad (3)$$

$$Sample_i^{(j)} = \Delta r^{(j)} + r^{(j)}(\Phi_k, \lambda_k, h_k) + \varepsilon_{Si} \qquad (4)$$

Image coordinates of GCPs are represented with $Line_i^{(j)}$ and $Sample_i^{(j)}$. The difference of the coordinates is calculated using the RPC based and reference coordinates and $\Delta p^{(j)}$ and $\Delta r^{(j)}$ are the functions of these differences. Coefficients obtained from the metadata file are used to generate the rational functions, $p^{(j)}(\Phi_k, \lambda_k, h_k)$ and $r^{(j)}(\Phi_k, \lambda_k, h_k)$.

The adjustment parameters are a_0, aS, aL, b_0, bL, bS, … terms in these equations.

Difference functions can be shown as:

$$\Delta p = a_0 + aS \,.\, Sample + aL \,.\, Line + aSL \,.\, Sample \,.\, Line + aL2 \,.\, Line^2 + aS2 \,.\, Sample^2 + \ldots \qquad (5)$$

$$\Delta r = b_0 + bS \,.\, Sample + bL \,.\, Line + bSL \,.\, Sample \,.\, Line + bL2 \,.\, Line^2 + bS2 \,.\, Sample^2 + \ldots \qquad (6)$$

3.5. Toutin's Model

The Toutin model is a physical model, in which the physical sensor parameters can be considered to generate collinearity equations that describe the relationship between 2D images and 3D objects. Toutin's model is one of these physical models to eliminate some errors caused by the physical parameters of the sensor. Even if the physical parameters are integrated, some distortions remain, such as inaccuracies in platform velocity and orientation, Earth curvature, integration time of the signal, and cartographic projection [27]. Image coordinates can be calculated by the equations below:

$$Pp + y(1 + \delta\gamma X) - \tau H - H_0 \Delta T^* = 0 \quad (7)$$

$$X + \theta H/\cos X + \alpha q(Q + \theta X - H/\cos X) - Q\Delta R = 0 \quad (8)$$

$$X = (x - ay)(1 + h/N_0) + by^2 + cxy \quad (9)$$

$$H = h - X^2/2N_0 \quad (10)$$

In the along-track and across-track directions, P and Q are the scale factors; correspondingly, p and q are the image coordinates, $\delta\gamma$, b, c and X are second-order variables, τ and θ are leveling angle functions in along-track and across-track directions, α is the field of view in real-time, x, y and h are ground coordinates, a is a function derived from a situation of non-perpendicularity in the axes, and finally N_0 is the distance of the normal to the ellipsoid.

3. Results

During the model testing, the use of various DEMs and GCP resources enabled us to investigate the effects of the DEM and GCP resources, and perform a comparative evaluation of the models. In addition, the models were applied using different numbers of GCPs, and the effect of the GCP number on the results was also examined. Except for the 2D Polynomial Model, which does not use a DEM as an input, 3 DEMs were integrated into each model. As the GCP resource, two datasets were used: Google Earth (GE) and the General Directorate of Mapping - Globe (HGM). In each GCP set, GCPs were selected homogeneously on the terrain. For accuracy assessment, 20 test points that were collected from the HGM Globe were used and kept constant for all models to ensure a fair comparison among different models.

4.1. Results of 2D Polynomial Model

The 2D polynomial models do not require elevation information. Thus, the effects of GCPs quantity and source of GCPs were tested by applying the model on PHR and SPOT images. To analyze the effects of GCP amount, we conducted geometric corrections with 20, 30, and 40 GCPs sets from each source (Table 1).

According to the RMSE results, the best results were obtained using 30 GCPs obtained from the HGM source for PHR and SPOT images. The RMSE values ranged between 9.2 to 10.5 meters for all GCP combinations from HGM, which were slightly better than the GCP combinations from GE. In all cases, total RMSE values are around 10m, and error values along X directions are higher than in Y direction in the 2D polynomial model

Table 1. RMSE table of the 2D polynomial model with different numbers of GCPs from GE and HGM. (Error values are in meters)

		GE		HGM	
		PHR	SPOT	PHR	SPOT
20 GCP	X	10.37	9.76	10.27	9.82
	Y	3.27	4.14	1.68	2.18
	Total	10.87	10.60	**10.40**	**10.06**
30 GCP	X	9.31	9.15	9.22	9.03
	Y	3.83	4.72	1.78	1.88
	Total	10.07	10.29	**9.39**	**9.22**
40 GCP	X	9.73	10.27	9.62	10.27
	Y	3.61	4.84	1.66	2.06
	Total	10.37	11.35	**9.76**	**10.47**

4.2. Results of 3D Rational Function Model with Calculated RPCs

In the 3D RFM model with calculated RPCs, the RPC coefficients were calculated with the use of GCPs but not RPC files provided with images. 3 DEMs were used to provide elevation information to GCPs and CPs. For this testing 40 GCPs - 20 coefficients, 30 GCPs-15 coefficients, and 20 GCPs - 10 coefficients setups were examined.

According to results for the SPOT image, the lowest RMSE values are obtained with ALOS DEM and HGM derived GCPs in all experiments. An increasing number of GCPs from 20 to 30 improved the results; whereas results are very similar to each other for 30 GCP and 40 GCP combinations (Table 2). Therefore, the usage of 30 GCPs would be a reasonable choice to minimize efforts. Integration of DEM and 3D RFM model provide similar error values along X and Y direction, which was not the case in 2D polynomials. Considering that GE is openly available and results of GE-based GCPs provided approximately 8m RMSE, GE might be a good alternative for those locations where other GCP sources are not available.

Table 2. RMSE table of RFM model of SPOT image with different DEMs and number of GCPs from GE and HGM. (Error values are in meters)

		SPOT - RFM - GE			SPOT - RFM - HGM		
		SRTM	ALOS	ASTER	SRTM	ALOS	ASTER
20 GCP	X	6.96	4.55	8.76	6.39	4.56	7.55
	Y	5.41	5.51	5.77	3.37	3.29	2.91
	Total	8.81	**7.15**	10.49	7.23	**5.62**	8.09
30 GCP	X	4.92	3.80	5.68	4.81	4.00	4.96
	Y	5.44	5.36	5.52	2.29	2.45	2.27
	Total	7.34	**6.57**	7.92	5.33	**4.69**	5.46
40 GCP	X	4.87	4.02	5.18	4.62	3.85	4.84
	Y	5.45	5.39	5.45	2.78	2.84	2.78
	Total	7.31	**6.72**	7.52	5.39	**4.78**	5.58

When the PHR results were examined in the tests of this model, it was observed that the accuracy was lower than the SPOT image, and the combination of HGM - 40

GCP - 20 RPC had large distortions in the model and increased RMSE values (Table 3). Less number of GCPs seems to be a better solution for the PHR case.

Table 3. RMSE table of RFM model of PHR image with different DEMs and number of GCPs from GE and HGM. (Error values are in meters)

		PHR - RFM - GE			PHR - RFM - HGM		
		SRTM	ALOS	ASTER	SRTM	ALOS	ASTER
20 GCP	X	2.20	2.12	2.97	4.47	5.49	4.35
	Y	7.70	8.30	7.53	3.95	5.72	3.92
	Total	**8.00**	8.57	8.09	5.96	7.93	**5.86**
30 GCP	X	3.16	3.18	4.11	5.75	5.72	6.64
	Y	6.87	7.32	7.54	7.08	8.98	7.89
	Total	**7.56**	7.98	8.59	**9.12**	10.65	10.31
40 GCP	X	5.41	3.51	11.04	19.24	7.89	22.85
	Y	5.93	6.38	8.56	9.83	11.79	23.02
	Total	8.02	**7.28**	13.97	21.61	**14.18**	32.43

4.3. Results of 3D Rational Functional Model with RPCs From Satellite

RFM model with original RPCs was applied to compare calculated RPCs and original RPCs results. 20 coefficients which were taken from SPOT and PHR imageries' RPC files were used and accuracy was tested via RMSE of 20 constant CPs. GCPs were not used in this model.

According to the results obtained by applying the 3D RFM model with the original RPC coefficients coming from the sensor, the DEM from the ALOS source gave more successful results in both images. The lowest RMSE in this model was obtained with the ALOS - PHR combination and is 2.38 meters (Table 3).

The RMSE values illustrate that RPC coefficients provided by Airbus are quite reliable and highly accurate ortho-rectified images could be generated by using RPCs without the need of GCPs.

Table 4. RMSE table of RFM model with original RPCs. (Error values are in meters)

	RFM with Original RPCs								
	ALOS			ASTER			SRTM		
(m)	X	Y	Total	X	Y	Total	X	Y	Total
PHR	1.60	1.77	**2.38**	2.17	1.78	**2.81**	1.71	1.74	**2.44**
SPOT	4.38	1.84	4.75	4.87	1.81	5.19	4.58	1.80	4.92

4.4. Results of RPC Refinement Model Using GCPs

The goal of the RPC refinement model was to evaluate how much the accuracy of the original RPCs from the satellite could be improved. For this purpose, 8 GCPs from 2 different sources were used for this improvement.

According to the application of the RPC Refinement model for SPOT image, 2nd degree was more successful when GE originated points were used, and 0^{th} degree when HGM originated points were used. The lowest RMSE in this image is obtained from the combination of HGM - ASTER with 4.06 meters (Table 5).

Table 5. RMSE table of RPC Refinement model of SPOT image with GCPs from Google Earth. with different DEMs and GCPs from GE and HGM. (Error values are in meters)

		SPOT - RPC REFINEMENT - GE			SPOT - RPC REFINEMENT - HGM		
		Adj Ord - 0	Adj Ord - 1	Adj Ord - 2	Adj Ord - 0	Adj Ord - 1	Adj Ord - 2
ALOS	X	3.62	3.63	3.62	3.67	3.78	3.84
	Y	5.01	5.07	4.33	1.90	2.06	2.08
	Total	6.18	6.24	5.64	4.13	4.30	4.36
ASTER	X	3.58	3.62	3.57	3.58	3.75	3.78
	Y	4.98	5.04	4.29	1.91	2.07	2.07
	Total	6.13	6.20	5.58	4.06	4.28	4.31
SRTM	X	4.07	4.09	4.14	4.11	4.14	4.23
	Y	5.02	5.08	4.33	1.85	1.99	2.00
	Total	6.46	6.52	5.99	4.50	4.60	4.67

Table 6. RMSE table of RPC Refinement model of PHR image with GCPs from Google Earth. with different DEMs and GCPs from GE and HGM. (Error values are in meters**)**

		PHR - RPC REFINEMENT - GE			PHR - RPC REFINEMENT - HGM		
		Adj Ord - 0	Adj Ord - 1	Adj Ord - 2	Adj Ord - 0	Adj Ord - 1	Adj Ord - 2
ALOS	X	1.60	1.71	1.69	1.80	1.80	1.80
	Y	2.02	2.03	2.15	1.31	1.44	1.47
	Total	2.58	2.65	2.73	2.23	2.30	2.32
ASTER	X	2.15	2.25	2.24	2.05	2.12	2.10
	Y	1.97	2.01	2.14	1.30	1.42	1.45
	Total	2.91	3.02	3.10	2.43	2.55	2.55
SRTM	X	1.77	1.88	1.89	1.59	1.59	1.63
	Y	1.98	2.00	2.13	1.34	1.45	1.47
	Total	2.66	2.75	2.85	2.08	2.15	2.20

The best results for the PHR image were observed with Adjustment Order - 0. Among all combinations, the lowest RMSE was obtained with the combination of SRTM DEM, and HGM based GCPs as 2.08 meters (Table 6).

4.5. Results of Toutin's Model

Toutin's Model was performed on two images using 8 GCPs from two different sources. While applying this model, three different DEMs were used to obtain elevations of GCPs. Thus, three different parameters were tested: terrain characteristics, effects of GCP sources and effects of DEM sources. It is also aimed to examine the differences between empirical and physical models in this step.

As a result of applying the Toutin Model, which is the only physical model in this study, the best results for the PHR image were obtained by using ALOS DEM. For the SPOT image, ASTER DEM provided slightly better results. One highlight here is that the PHR-ALOS and SPOT-ASTER combinations gave the highest accuracy in both GCP sources. The best result in this model was obtained at 3.21 meters with the combination of PHR - ALOS DEM and GE-based GCPs.

Table 7. RMSE table of Toutin's model with GCPs from GE and HGM. (Error values are in meters)

		TOUTIN - GE		TOUTIN - HGM	
		PHR	SPOT	PHR	SPOT
ALOS	X	1.76	3.27	1.94	3.88
	Y	2.69	3.86	2.92	2.14
	Total	**3.21**	5.06	**3.51**	4.43
ASTER	X	2.28	3.18	2.36	3.71
	Y	2.72	3.89	2.99	2.15
	Total	**3.55**	5.02	**3.80**	4.29
SRTM	X	2.11	3.74	2.07	4.20
	Y	2.71	3.91	2.91	2.12
	Total	**3.43**	5.41	**3.57**	4.71

4. Discussion

According to the accuracy assessment results, the best results were obtained with RFM modeling, which used RPC from the data provider for both PHR and SPOT images. The GCPs derived from the HGM source provided lower RMSE values when compared to GCPs from GE. The analysis with different numbers of GCPs provided that increasing the number from 20 to 30 provided improvement in accuracy; however, further increment to 40 GCPs did not help improvement, and even lowered the performance in some experiment setups. In terms of DEM data contribution, in most of the experiments, better results were obtained using ALOS DEM. The experiments on the PHR image provided lower RMSE values except for the RFM modeling with calculated RPCs, where a significant bias is observed in the Y direction. Toutin physical model and RFM modeling with RPCs from the data provider were found to be the most stable geometric correction methods considering various DEMs and GCP sources. Toutin model provided very close results for different DEMs for both GCP data sources. This showed the fidelity of the physical model even with different cases in which different accuracy DEMs and GCPs were used. It can be inferred that, Toutin model could be reliably applied to different regions by using open-source DEMs and GE GCPs. Moreover, in case of not having reliable RPC files from the data provider, Toutin physical model will be a good alternative for the geometric correction.

5. Conclusion

Extracting accurate and reliable locational information from satellite images require efficient geometric correction procedure. In this study, we comparatively evaluated five different geometric correction methods with various experimental designs including different GCP sources and numbers, multi-source DEMs over the Pleiades and SPOT 6 satellite images with different spatial resolutions. Lower RMSE values were obtained with the model that uses RPC from data providers for PHR and SPOT, followed by the RPC refinement method for PHR and the Toutin method for SPOT. GCPs from the HGM data source and the ALOS DEM combination produced better results in general. Finally, with the exception of one test, the PHR image has lower RMSE values and thus better locational accuracies. Toutin model is a good solution for geometrically correcting the satellite images without RPC files.

Acknowledgement

Authors acknowledge the support of ITU-CSCRS for providing Pleiades and Spot 6 satellite images.

Author contributions

Buğrahan Özcihan: Methodology, Analysis, Writing-Original draft preparation **Levent Doğukan Özlü:** Methodology, Analysis, Writing-Original draft preparation **Mümin İlker Karakap:** Methodology, Analysis, Writing-Original draft preparation **Halime Sürmeli:** Methodology, Analysis, Writing-Original draft preparation **Ugur Alganci:** Methodology, Visualization, Investigation, Writing-Reviewing and Editing **Elif Sertel:** Supervision, Methodology, Visualization, Writing-Reviewing and Editing

Conflicts of interest

The authors declare no conflicts of interest.

References

1. Bai, X., Zhang, H., & Zhou, J. (2014). VHR object detection based on structural feature extraction and query expansion. IEEE Transactions on Geoscience and Remote Sensing, 52, 6508–6520.
2. Joshi, N., Baumann, M., Ehammer, A., Fensholt, R., Grogan, K., Hostert, P., Jepsen, M.R., Kuemmerle, T., Meyfroidt, P., Mitchard, E.T.A., Reiche, J., Ryan, C.M., & Waske, B. (2016). A review of the application of

optical and radar remote sensing data fusion to land use mapping and monitoring, Remote Sensing, 8(1), 70.
3. Göksel, Ç. & Bozkaya Karip, G. (2017). İğneada Koruma Alanının Arazi Örtüsü/Arazi Kullanımının Zamana Bağlı Değişiminin Markov Zincirleri İle Modellenmesi. Geomatik, 2 (2), 94-105.
4. Durkut, Z., Algancı, U. & Sertel, E. (2020). Uydu Görüntüsü İşleme ve Sıkıştırma Süreçlerinin WEB Tabanlı Harita Servisi Yayın Performansına Etkilerinin Araştırılması. Geomatik, 5 (3), 186-192.
5. Zabcı, C. (2021). Çok bantlı Landsat 8-OLI ve Sentinel-2A MSI uydu görüntülerinin karşılaştırmalı jeoloji uygulaması: Örnek çalışma alanı olarak Doğu Anadolu Fayı boyunca Palu – Hazar Gölü bölgesi (Elazığ, Türkiye). Geomatik, 6 (3), 238-246.
6. Karagianni, A. (2022). Road extraction through digital processing and visual interpretation of satellite images. International Journal of Engineering and Geosciences, 7 (3), 264-271.
7. Guha, S. & Govil, H. (2022). Estimating the seasonal relationship between land surface temperature and normalized difference bareness index using Landsat data series. International Journal of Engineering and Geosciences, 7 (1), 9-16.
8. Paul, S. (2022). Change detection and future change prediction in Habra I and II block using remote sensing and GIS – A case study. International Journal of Engineering and Geosciences, 7 (2), 191-207.
9. Saroğlu, E. (2004). Farklı çözünürlükteki uydu görüntülerinin geometrik dönüşümü ve dönüşüm sonucunda elde edilen görüntülerin dış doğruluğunun araştırılması (Master of Science dissertation, Fen Bilimleri Enstitüsü).
10. Sertel, E., Kutoglu, S. H., & Kaya, S. (2007). Geometric correction accuracy of different satellite sensor images: Application of figure condition. International Journal of Remote Sensing, 28, 4685–4692.
11. Kartal, H., Alganci, U., & Sertel, E. (2018). Automated orthorectification of VHR satellite images by SIFT-based RPC refinement. ISPRS International Journal of Geo-Information, 7(6), 229.
12. Toutin, T. (2003). Geometric correction of remotely sensed images. In Remote Sensing of Forest Environments (pp. 143-180). Springer, Boston, MA.
13. Toutin, T. (2004). Geometric processing of remote sensing images: Models, algorithms and methods. International Journal of Remote Sensing, 25, 1893–1924.
14. Alganci, U., Besol, B., & Sertel, E. (2018). Accuracy assessment of different digital surface models. ISPRS International Journal of Geo-Information, 7(3), 114.
15. Zhang, Ying, Zhaohui Chi, Fengming Hui, Teng Li, Xuying Liu, Baogang Zhang, Xiao Cheng, and Zhuoqi Chen. (2021). Accuracy Evaluation on Geolocation of the Chinese First Polar Microsatellite (Ice Pathfinder) Imagery. Remote Sensing, 13(21), 4278.
16. Samadzadegan, F., Milanlak, A., & Majdabadi, M. (2006). Geometrical Correction of Satellite Images by Generic Models. In Proceedings of the ISPRS Commission VII Symposium 'Remote Sensing: From Pixels to Processes', Enschede, Netherlands, (pp. 1-5)
17. Ye, J., Lin, X., & Xu, T. (2017). Mathematical modeling and accuracy testing of worldview-2 level-1B stereo pairs without ground control points. Remote Sensing, 9(7), 737.
18. Son, J.-H., Yoon, W., Kim, T., & Rhee, S. (2021). Iterative Precision Geometric Correction for High-Resolution Satellite Images. Korean Journal of Remote Sensing, 37(3), 431–447.
19. Mezouar, O., Meskine, F., Boukerch, I. & Taleb N (2021). A Hybrid particle swarm optimization of the rational function model for satellite strip images ortho-rectification. International Journal of Remote Sensing, 42(21), 8056-8076.
20. Misra, I., Rohil, M. K., Moorthi, S. M. & Dhar, D. (2022). FIRM: Framework for Image Registration Using Multistage Feature Detection and Mode-Guided Motion Smoothness Keypoint Optimization. IEEE Transactions on Geoscience and Remote Sensing, 60, 1-12.
21. Wang, T., Li, X., Zhang, G., Lin, M., Deng, M., Cui, H., Jiang, B., Wang, Y., Zhu, Y., Wang, H. & Yuan, X. (2022). Large-Scale Orthorectification of GF-3 SAR Images Without Ground Control Points for China's Land Area. IEEE Transactions on Geoscience and Remote Sensing, 60, 1-17, 5221617
22. Shaker, A., Shi, W., & Barakat, H. (2005). Assessment of the rectification accuracy of IKONOS imagery based on two-dimensional models, International Journal of Remote Sensing, 26(4), 719-731
23. PCI Geomatics. (2012). Geomatica Help. PCI Geomatics: Markham, ON, Canada.
24. Tao, V., & Hu, Y. (2001). A Comprehensive Study of the Rational Function Model for Photogrammetric Processing. Photogrammetric Engineering & Remote Sensing, 67(12), 1347 – 1357.
25. Grodecki, J. (2001). Ikonos Stereo Feature Extraction-RPC Approach. Annual Conference of the ASPRS 2001, St. Louis, 23-27 April 2001
26. Hu, Y., Tao, V., Croitoru, A. (2004). Understanding the rational function model: Methods and applications. International Archives of Photogrammetry and Remote Sensing 20, 119–124.
27. Toutin, T. (1995). Generating DEM from stereo-images with a photogrammetric approach: examples with VIR and SAR data. EARSeL Advances in Remote Sensing, 4, 110–117.